International Atomic Energy Agency

INDC(BZL)-17
Distr.: G

INDC INTERNATIONAL NUCLEAR DATA COMMITTEE

GENERATION OF ELASTIC AND DISCRETE INELASTIC TRANSFER MATRICES

R.D.M. Garcia and M.D. Santina

Aerospace Technical Centre
Institute of Advanced Studies
12 200 Sao José dos Campos
Sao Paulo, Brazil

English translation of the Brasilian research report
IEAv-08/85
Translated by IAEA, May 1985

IAEA NUCLEAR DATA SECTION, WAGRAMERSTRASSE 5, A-1400 VIENNA

Printed by the International Atomic Energy Agency
Vienna, Austria

INDC(BZL)-17
Distr.: G

GENERATION OF ELASTIC AND DISCRETE INELASTIC TRANSFER MATRICES

R.D.M. Garcia and M.D. Santina

Aerospace Technical Centre
Institute of Advanced Studies
12 200 Sao José dos Campos
Sao Paulo, Brazil

English translation of the Brasilian research report
IEAv-08/85
Translated by IAEA, May 1985

L85-12390
Translated from Portuguese

Research Report
IEAv-08/85
8 April 1985

GENERATION OF ELASTIC AND DISCRETE INELASTIC TRANSFER MATRICES

R.D.M. Garcia and M.D. Santina
Aerospace Technical Centre
Institute of Advanced Studies
Rodovia dos Tamoios, km 5.5
12 200 São José dos Campos
São Paulo, Brazil

ABSTRACT

The paper describes a technique developed for the calculation of the isotropic and linearly anisotropic components of elastic and discrete inelastic transfer matrices. Implementation of the technique is discussed in detail and the numerical data obtained for some examples are compared with results published in the literature or those generated with the help of several processing codes.

---

1. INTRODUCTION

In an earlier paper [1] a technique was proposed for the calculation of the isotropic ($k = 0$) and linearly anisotropic ($k = 1$) components of elastic and discretely inelastic transfer matrices, expressed by

$$\sigma_x \; (g' \to g, \; k) = W_{g'}^{-1} \int_{E^*_{g'}}^{E^*_{g'-1}} dE' \; W(E') \quad \sigma_x(E') \; F_k(E', g) \quad , \tag{1}$$

where g' represents the initial group, with $E' \epsilon (E_{g'}, E_{g'-1})$; g is the final group, with $E \epsilon (E_g, E_{g-1})$; $\sigma_x(E')$ is the cross-section for the scattering mechanism x at energy E', and W(E') is the weighting function with $W_{g'}$ given by the integral of W(E') over group g'. The integration limits are given by $E^*_{g'} = \max(E_{g'}, E_\ell)$ and $E^*_{g'-1} = \max(E_{g'-1}, E_\ell)$, where E_ℓ represents the threshold scattering energy and the function $F_k(E', g)$ is expressed by [1]

$$F_k(E',g) = \frac{1}{2} \sum_{\ell=0}^{L} (2\ell+1) \; f_x(E',\ell) \; X_{k,\ell}(E',g) \quad , \tag{2}$$

where $f_x(E', \ell)$, with $f_x(E', 0) = 1$, are the expansion coefficients for the angular distribution of the scattered neutrons in the Legendre polynominals $P_\ell(\omega)$, and $X_{k,\ell}(E',g)$ are the angular integrals [1] which can be calculated efficiently by a semi-analytical technique [2] developed for $k = 0$ and 1.

In Section 2 we describe an algorithm developed specially for performing the integration over the energy indicated in Eq. (1) in an efficient and accurate manner. Although apparently trivial from the numerical point of view, the above integration involves subtle aspects which, if not properly considered, can appreciably affect the final accuracy of the results. In Section 3 we study several examples, give numerical results and compare them with data obtained by other methods. Section 4 summarizes the principal conclusions of the study.

It is important to point out that in the present paper we consider only the smooth component of the cross-section; the resonant component can be treated similarly after it is linearized.

2. ALGORITHM FOR ENERGY INTEGRATION

The integrand in Eq. (1) consists of a product of three quantities, of which two make use of nuclear data supplied by evaluated data libraries, such as ENDF/B [3]: cross-section $\sigma_x(E')$ is given in file 3 of ENDF/B in the form of pairs of points $(E_i,\sigma_x(E_i)]$ with a specified interpolation scheme, and the function $F_k(E',g)$, in accordance with Eq. (2), uses coefficients $f_x(E',\ell)$ supplied from file 4 of ENDF/B in the form $[E_j,f_x(E_j,\ell)]$, where $\ell = 1,2, \ldots,L \leq 20$ with a specified energy interpolation scheme. It is clear that this representation normally introduces discontinuities into the derivative of $\sigma_x(E')$ at points $\{E_i\}$ and into the derivative of $F_k(E',g)$ at points $\{E_j\}$. The third quantity appearing in the integrand of Eq. (1), the weighting function $W(E')$, can also be used, for convenience, in the form of pairs of points $[E_k,W(E_k)]$ with a specified interpolation scheme. Consequently, the derivativ of $W(E')$ may be discontinuous at points $\{E_k\}$.

Function $F_k(E',g)$ can have still other discontinuities in its derivative, which originate from the angular integrals $X_{k,\ell}(E',g)$. In order to explain the origin of these discontinuities, we should note that by definition [1]

$$X_{k,\ell}(E',g) = \int_{\omega_g(E')}^{\omega_{g-1}(E')} d\omega\, P_k \{[1 + \gamma(E')\omega]\,[1+2\gamma(E')\omega+\gamma^2(E')]^{-1/2}\} P_\ell(\omega), \qquad (3)$$

where ω is the cosine of the scattering angle in the centre-of-mass system, and the

the angular integrals depend basically on the integration limits $\omega_g(E') = \max \{-1, \min [\omega(E_g,E'),1]\}$ and $\omega_{g-1}(E') = \min \{1, \max [\omega (E_{g-1},E'), -1]\}$, where

$$\omega(E,E') = \frac{1}{2} \{[(A+1)^2 \frac{E}{E'} -1] \frac{1}{\gamma(E')} - \gamma(E')\} \quad . \tag{4}$$

The parameter $\gamma(E')$ appearing in Eqs (3) and (4) is given by

$$\gamma(E') = A \left(1 + \frac{A+1}{A} \frac{Q_i}{E'}\right)^{1/2} , \tag{5}$$

where A is the ratio between the mass of the scattering nucleus and that of the neutron, and $Q_i \leq 0$, $i = 0, 1, \ldots, I$, is the excitation energy at level i of the scattering nucleus, with $Q_0 = 0$ representing elastic scattering. Thus, a possible discontinuity in the derivative of any one of the integration limits of Eq. (3) in relation to E' will cause a discontinuity in the derivative of $X_{k,\ell}(E',g)$. As an example of this type of discontinuity, we can see in Fig. 1 a point of discontinuity in the derivative of $X_{k,\ell}(E',g)$ which occurs in the calculation of elastic transfer of group 5 (9.0484-10 MeV) of the GAM-II structure [4] for the same group in ^{27}Al. This discontinuity, indicated by point P, is produced by the one in the derivative of the lower limit $\omega_g(E')$ at E' = 9.7512 MeV.

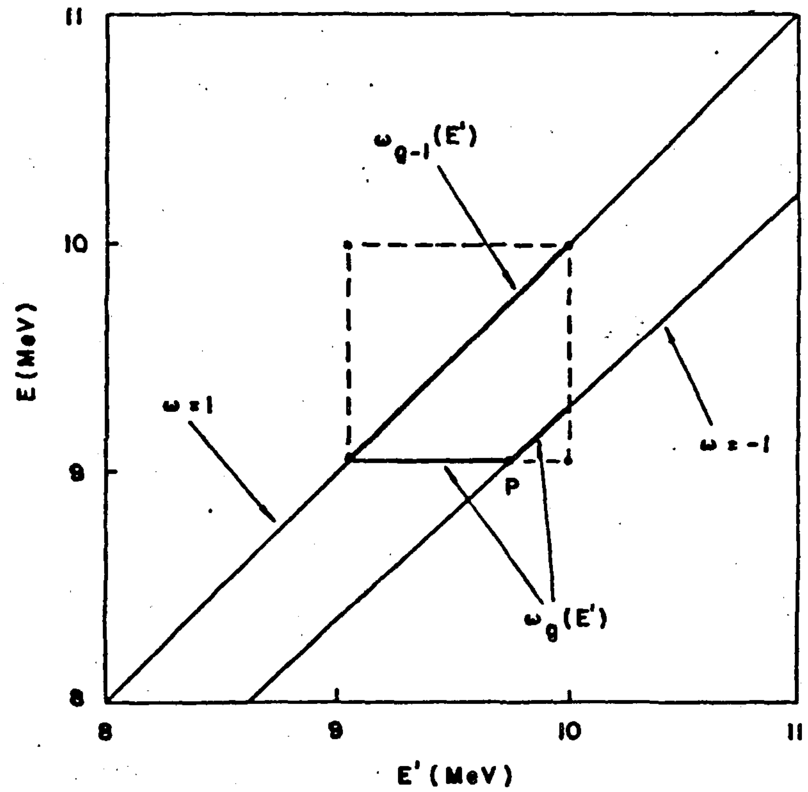

Fig. 1. Example of discontinuity in the derivative of $\omega_g(E')$ for ^{27}Al.

A simple way of avoiding these discontinuities is to sub-divide the energy integration interval in Eq. (1) in a manner such that within each sub-division the integrand of Eq. (1) and its derivative are continuous. Thus, Eq. (1) is written initially as

$$\sigma_x(g' \to g,k) = W_{g'}^{-1} \sum_{m=1}^{M} \int_{E_m(g',g)}^{E_{m+1}(g',g)} dE' \; W(E') \; \sigma_x(E') \; F_k(E',g) \quad , \tag{6}$$

where $E_m(g',g)$, m = 1,2, ..., M + 1, are the limits of the sub-intervals located in M + 1 possible discontinuities of the derivative of $X_{k,\ell}(E',g)$. To locate these discontinuities, we have to determine the points of intersection between the sides of the rectangle with vertices $(E^*_{g'},E_g)$, $(E^*_{g'-1},E_g)$, $(E^*_{g'},E_{g-1})$ and $(E^*_{g'-1},E_{g-1})$ and the curves

$$E = \frac{E'}{(A+1)^2} \left[1 \pm \gamma(E')\right]^2 \tag{7}$$

in the plane (E',E). The results of this analysis are presented below.

<u>Case 1</u>:

$$E^*_{g'} \geq -\left(\frac{A}{A-1}\right) Q_i \; .$$

$$E_1(g',g) = \max \{E^*_{g'}, \min [E^*_{g'-1}, \Gamma(E_g, 1)]\} \quad , \tag{8a}$$

$$E_2(g',g) = \min \{a, b\} \quad , \tag{8b}$$

$$E_3(g',g) = \max \{a, b\} \quad , \tag{8c}$$

$$E_4(g',g) = \min \{E^*_{g'-1}, \max [E^*_{g'}, \Gamma(E_{g-1}, -1)]\} \quad , \tag{8d}$$

where

$$a = \max \{E^*_{g'}, \min [E^*_{g'-1}, \Gamma(E_{g-1}, 1)]\} \quad , \tag{9a}$$

$$b = \min \{E^*_{g'-1}, \max [E^*_{g'}, \Gamma(E_g, -1)]\} \tag{9b}$$

and

$$\Gamma(E,\omega) = \frac{E}{(A-1)^2} \left\{ \frac{A^2 - 1 - A(A-1)Q_i/E}{[A^2 - 1 - A(A-1)Q_i/E + \omega^2]^{1/2} + \omega} \right\}^2 . \tag{10}$$

Case 2a: $E^*_{g'} < -\left(\frac{A}{A-1}\right) Q_i$ e $E_g > -\frac{Q_i}{A(A+1)}$.

The results are identical with those of Case 1.

Case 2b:

$$E^*_{g'} < -\left(\frac{A}{A-1}\right) Q_i \quad e \quad E_{g-1} \leq -\frac{Q_i}{A(A+1)} \quad .$$

$$E_1(g',g) = \max \{E^*_{g'}, \min [E^*_{g'-1}, \Gamma(E_{g-1}, 1)]\} \quad , \tag{11a}$$

$$E_2(g',g) = \max \{E^*_{g'}, \min [E^*_{g'-1}, \Gamma(E_g , 1)]\} \quad , \tag{11b}$$

$$E_3(g',g) = \min \{E^*_{g'-1}, \max [E^*_{g'} , \Gamma(E_g, -1)]\} \quad , \tag{11c}$$

$$E_4(g',g) = \min \{E^*_{g'-1}, \max [E^*_{g'}, \Gamma (E_{g-1}, -1)]\} \quad . \tag{11d}$$

Case 2c:

$$E^*_{g'} < -\left(\frac{A}{A-1}\right) Q_i , E_{g-1} > -\frac{Q_i}{A(A+1)} \quad e \quad E_g < -\frac{Q_i}{A(A+1)} \quad .$$

$$E_1(g',g) = E^*_{g'} \quad , \tag{12a}$$

$$E_2(g',g) = \min \{c, d\} \quad , \tag{12b}$$

$$E_3(g',g) = \max \{c, d\} \quad , \tag{12c}$$

$$E_4(g',g) = \min \{E^*_{g'-1} , \Gamma (E_g , -1)\} \quad , \tag{12d}$$

$$E_5(g',g) = \min \{E^*_{g'-1} , \Gamma (E_{g-1} , -1)\} \tag{12e}$$

where

$$c = \max \{E^*_{g'} , \min [E^*_{g'-1} , \Gamma (E_{g-1} , 1)]\} \tag{13a}$$

and

$$d = \max \{E^*_{g'} , \min [E^*_{g'-1} , \Gamma (E_g , 1)]\} \quad . \tag{13b}$$

Each of the M sub-intervals is then divided as many times as are necessary so that the limits of each of their sub-divisions are the points of discontinuity $\{E_i\}$, $\{E_j\}$ and $\{E_k\}$ which may be present within the sub-interval. In this manner, the discontinuities in the derivatives of $\sigma_x(E')$, $f_x(E',\ell)$ and, possibly, $W(E')$ are avoided. Lastly, integration of Eq. (1) is carried out with the use of a low-order Gauss-Legendre quadrature in each of the sub-divisions of each sub-interval.

3. NUMERICAL EXAMPLES

A program called TRAMA has been written and implemented in the CYBER 170/750 system of the Institute of Advanced Studies (Aerospace Technical Centre) in order to test the algorithm described in section 2. Several examples treated earlier in the literature were used, and the results obtained with the TRAMA program were compared with those of several processing codes. Although the numerical accuracy required for the transfer matrices is in practice much lower than that obtained with the TRAMA program in the examples studied (5 significant digits), we consider it important to provide results with this degree of accuracy for two reasons: first, the search for results of high accuracy may reveal possible programming errors which are difficult to detect and, second, publication of accurate results for well-defined problems facilitates comparison with results obtained by other methods. The necessary nuclear data were obtained from the ENDF/B library, version IV [3].

3.1. Inelastic scattering of ^{16}O

This example was used by Brockmann to test the TRACS program [5]. It involves calculating the inelastic scattering matrix involving the first excited level (Q_1 = -6.052 MeV) of ^{16}O (MAT = 1276) for the first 12 groups of the fine structure of the GAM-II code [4] with the weighting function of the form 1/E. The limits of each energy group considered were obtained by rounding off the values published in Ref. [4] to four decimal places, and are given explicitly in Ref. [5].

In Tables 1 and 2 the results obtained with the use of four points of quadrature per sub-division in the TRAMA program for the isotropic and linearly anisotropic components of the inelastic transfer matrix of ^{16}O are compared with the results of several processing codes. It is noted that the results of TRAMA and NJOY [6] show satisfactory agreement, the maximum relative deviation observed in NJOY being 0.19%. As for the results of XLACS [7] and ETOG3 [8], owing to the simplicity of the models adopted in these codes for describing the discrete inelastic scattering mechanism [9], they exhibit, as is expected, quite high deviations as compared with the more accurate results of TRAMA and NJOY. The agreement between the results published by Brockmann [5] and those of the TRAMA program is excellent.

3.2. Inelastic scattering of ^{7}Li

This example consists of calculating the inelastic scattering matrix for the first excited level (Q_1 = -0.478 MeV) of ^{7}Li (MAT = 1272) with the same group structure and weighting function as in the preceding example. Numerical results for this example were published by Hong and Shultis [10] for several transfer matrix components between groups 1 and 5 of the above-mentioned structure, but with group energy values differing slightly from those used in the preceding example owing to the application of a different rounding-off criterion on the values published in Ref. [4].

In Tables 3 and 4 the results obtained with the use of four points of quadrature per sub-division in the TRAMA program for the isotropic and linearly anisotropic components of the inelastic transfer matrix of ^{7}Li for the first two energy groups of the structure considered are compared with those of several processing codes. As in the preceding example, the results of TRAMA and NJOY show satisfactory agreement (maximum relative deviation 0.17%), and the difference observed with respect to the results of the XLACS and ETOG3 codes is still more evident since the simplified models adopted in those codes for inelastic scattering do not give good results when applied to light nuclei. An additional comparison using the TRAMA program with group energy values exactly the same as those in Ref. [10] resulted in perfect agreement for the component $\sigma_x(1 \rightarrow 5,0)$ obtained with the TRAMA program and the best value reported in Ref. [10], while the component $\sigma_x(1 \rightarrow 5, 1)$ showed a difference of only 1 in the fifth significant digit, considering a factor of 3, since the results reported in Ref. [10] are multiplied by $2\ell + 1$.

3.3 Elastic scattering of ^{239}Pu

This example was used by Henryson and co-workers [11] in the evaluation of some computational methods available in the MC^2-2 code [12]. It consists in calculating the elastic scattering matrix of ^{239}Pu, with a constant weighting function, for some groups of the ultra-fine structure [13] of the MC^2 code shown in Table 5.

In Tables 6 and 7 the results obtained with the use of eight points of quadrature per sub-division in the TRAMA program for the isotropic and linearly anisotropic components of the elastic transfer matrix of ^{239}Pu are compared with the results of NJOY, XLACS and MC^2. The TRAMA and NJOY results again display satisfactory agreement (maximum relative deviation 0.28%). The results of the XLACS code obtained with the use of 20 points in the initial group and 40 in the final group are lower, while those of the MC^2 code differ from the values found with TRAMA and NJOY, as was expected. Since the version of the ENDF/B library used to obtain the results published in Ref. [11] was older than version IV, it was not possible to compare it with those results.

3.4. Elastic scattering of ^{27}Al

This example was used by Weisbin and co-workers [14] in the evaluation of the MINX code [15]. It consists in calculating the elastic scattering matrix of ^{27}Al in a structure with 11 groups in the 0.414 eV-10 MeV range and a tabulated weighting function, which are given in Ref. [14].

In Tables 8 and 9 the results obtained with the use of four points of quadrature per sub-division in the TRAMA program for the isotropic and linearly anisotropic components of the elastic transfer matrix of ^{27}Al are compared with the NJOY and XLACS results. The agreement between the TRAMA and NJOY results is excellent (maximum relative deviation 0.03%). As for the XLACS results, although they were obtained with the use of 80 points in the initial group and 160 in the final group, they exhibit much greater deviations - above 10% for some of the values shown in Tables 8 and 9.

4. CONCLUSIONS

The results obtained by the TRAMA program in the case of the examples shown in the preceding section lead to the conclusion that the technique described in this paper can supply numerical results with high accuracy for the isotropic and linearly anisotropic components of the elastic and discrete inelastic transfer matrices. Thus, the technique can be used, as in the present study, to produce reference numerical results for selected problems, and this facilitates evaluation of the accuracy of the existing processing codes. Of the codes considered in the present work, the NJOY system undeniably provided the best results, even though some anomalies were detected in the scattering matrices for the higher- and lower-energy groups. These difficulties were brought to the notice of those responsible for the code.

In terms of processing time, although the angular integration algorithm used in the TRAMA program is generally faster than the numerical integration used in NJOY [2], we observed that the processing times for TRAMA were longer than those for NJOY (but shorter than for XLACS). The reason is that the algorithm for integration over the initial energy in TRAMA uses a separate energy grid for E' for each final group so as to avoid the discontinuities in the derivative of $X_{k,\ell}(E',g)$, which were discussed in Section 2. The NJOY system, however, does not distinguish between the various final groups and uses the same energy grid for E' in all cases. This undoubtedly makes the NJOY execution time faster, although the reliability of the results is lower as a result of the NJOY algorithm being mathematically less rigorous.

For example, as regards the generation of transfer matrices for discrete inelastic scattering, it was found that codes which did not take account of angular distribution of scattered neutrons, such as the XLACS and ETOG3 programs used in this study, gave results with large deviations from the correct values, especially for light nuclei. The influence of the approximations used by these codes on the reactivity and some of the spectral indices for certain fast systems has been analysed [16]; however, a fuller study of these effects would be highly desirable.

Lastly, after generalization with a view to its application to resonances and processing of all possible representations in ENDF/B file 4, the technique discussed in this paper can be easily implemented, replacing older techniques which are used in the existing processing codes, or be incorporated into the new processing code which is being developed at the Nuclear Data Centre of the Institute of Advanced Studies.

ACKNOWLEDGEMENTS

The authors wish to express their thanks to J. Anaf, S. Bogado Leite, E.S. Chalhoub and R.P. Kesavan Nair for discussion of various aspects of this study and for their help in the use of the processing codes.

REFERENCES

[1] GARCIA, R.D.M., A New Technique for Generation of Transfer Matrices for Elastic and Discrete Inelastic Scattering. Technical Report IEAv/NT-010/84, Institute of Advanced Studies (1984) (in Portuguese).

[2] GARCIA, R.D.M., A Study of the Computational Efficiency of a Semi-analytical Technique for Evaluation of Angular Integrals Found in the Generation of Transfer Matrices. Technical Report IEAv/NT-011/84, Institute of Advanced Studies (1984) (in Portuguese).

[3] GARBER, D., DUNFORD, C. and PEARLSTEIN, S., Data Formats and Procedures for the Evaluated Nuclear Data File, ENDF, BNL-NCS-50496, Brookhaven National Laboratory, 1975.

[4] JOANOU, G.D. and DUDEK, J.S.,"GAM-II: A B_3 Code for the Calculation of Fast-Neutron Spectra and Associated Multigroup Constants", GA-4265, General Atomic, 1963.

[5] BROCKMANN, H., Atomkernenergie-Kerntechnik, 35 (1980) 15-19.

[6] MACFARLANE, R.E., MUIR, D.W. and BOICOURT, R.M., The NJOY Nuclear Data Processing System, Volume I: User's Manual, LA-9303-M, Los Alamos National Laboratory, 1982.

[7] GREENE, N.M., LUCIUS, J.L., WHITE, J.E., WRIGHT, R.Q., CRAVEN, C.W. Jr., TOBIAS, M.L., XLACS: A Program to Produce Weighted Multigroup Neutron Cross-Sections from ENDF/B, ORNL - TM - 3646, Oak Ridge National Laboratory, 1972.

[8] BOGADO LEITE, S.Q., Use of the ETOG3 Code in the Preparation of Epithermal Library for HAMMER with ENDF/B-IV Data. Informal Report NI/ENU/001/83, Institute of Advance Studies (1983) (in Portuguese).

[9] GARCIA, R.D.M., Review of the Methods of Transfer Matrix Generation in Computational Codes Based on the ENDF/B Data Library. Internal Report IEAv/RI-008/84. Institute of Advanced Studies (1984) (in Portuguese).

[10] HONG, K.J., SHULTIS, J.K., Nucl. Sci. Eng., 80 (1982) 570-578.

[11] HENRYSON II, H., STENBERG, C.G., TOPPEL, B.J., Calculation of Elastic Scattering Matrices, Applied Physics Division Annual Report, 1 July 1969 to 30 June 1970, ANL - 7710, Argonne National Laboratory (1971).

[12] HENRYSON II, H., TOPPEL, B.J., STENBERG, C.G., MC^2-2: A Code to Calculate Fast Neutron Spectra and Multigroup Cross-Sections, ANL - 8144, Argonne National Laboratory (1976).

[13] TOPPEL, B.J., RAGO, A.L., O'SHEA, D.M., MC^2, A Code to Caculate Multigroup Cross-Sections, ANL - 7318, Argonne National Laboratory (1967).

[14] WEISBIN, C.R., SORAN, P.D., HENDRICKS, J.S., Nucl. Sci. Eng., 55 (1974) 329-341.

[15] WEISBIN, C.R., SORAN, P.D., MACFARLANE, R.E., HARRIS, D.R., LABAUVE, R.J., HENDRICKS, J.S., WHITE, J.E., KIDMAN, R.B., MINX: A Multigroup Interpretation of Nuclear X-Sections from ENDF/B, LA-6486-MS, Los Alamos Scientific Laboratory (1974).

[16] SEGEV, M., Nucl. Sci. Eng., 45 (1971) 269-278.

Table 1. The isotropic component $\sigma_x(g' \rightarrow g, 0)$ of the inelastic transfer matrix for the 6.052 MeV level of ^{16}O.

g'	g	TRAMA	NJOY	XLACS	ETOG-3
1	6	3,4629(-3)	3,462(-3)	0	0
1	7	1,2888(-2)	1,289(-2)	4,5789(-3)	5,0744(-3)
1	8	1,3103(-2)	1,310(-2)	2,2848(-2)	2,3517(-2)
1	9	8,2994(-3)	8,299(-3)	1,4635(-2)	1,3478(-2)
1	10	3,8343(-3)	3,833(-3)	0	0
1	11	4,8202(-4)	4,811(-4)	0	0
2	8	5,5013(-3)	5,506(-3)	0	0
2	9	1,3874(-2)	1,387(-2)	9,0062(-3)	1,0016(-2)
2	10	1,3821(-2)	1,382(-2)	2,4096(-2)	2,4722(-2)
2	11	9,8142(-3)	9,813(-3)	1,5779(-2)	1,4142(-2)
2	12	5,0077(-3)	5,006(-3)	0	0
3	9	1,6156(-5)	1,616(-5)	0	0
3	10	7,2168(-3)	7,219(-3)	0	0
3	11	2,1737(-2)	2,174(-2)	1,0929(-2)	1,7321(-2)
3	12	2,5913(-2)	2,591(-2)	4,2035(-2)	4,2600(-2)
4	12	4,4720(-3)	4,478(-3)	0	0

Table 2. The linearly anisotropic component $\sigma_x(g' \to g, 1)$ of the inelastic transfer matrix for the 6.052 MeV level of ^{16}O.

g'	g	TRAMA	NJOY
1	6	2,9883(-3)	2,988(-3)
1	7	8,5827(-3)	8,586(-3)
1	8	3,9849(-3)	3,983(-3)
1	9	-2,2956(-3)	-2,297(-3)
1	10	-2,5254(-3)	-2,525(-3)
1	11	-4,3297(-4)	-4,322(-4)
2	8	4,5548(-3)	4,558(-3)
2	9	8,5560(-3)	8,554(-3)
2	10	3,2986(-3)	3,297(-3)
2	11	-2,9485(-3)	-2,949(-3)
2	12	-3,2433(-3)	-3,242(-3)
3	9	1,6010(-5)	1,602(-5)
3	10	5,9871(-3)	5,989(-3)
3	11	1,4015(-2)	1,402(-2)
3	12	8,0943(-3)	8,090(-3)
4	12	3,7394(-3)	3,744(-3)

Table 3. The isotropic component $\sigma_x(g'\to g, 0)$ of the inelastic transfer matrix for the 0.478 MeV level of ^7Li.

g'	g	TRAMA	NJOY	XLACS	ETOG-3
1	1	3,8568(-3)	3,854(-3)	0	0
1	2	1,5730(-2)	1,574(-2)	0	0
1	3	1,5280(-2)	1,528(-2)	1,1772(-2)	1,2336(-2)
1	4	1,3826(-2)	1,383(-2)	6,8592(-2)	6,8029(-2)
1	5	1,2510(-2)	1,251(-2)	0	0
1	6	1,1320(-2)	1,132(-2)	0	0
1	7	7,4754(-3)	7,476(-3)	0	0
1	8	3,6551(-4)	3,649(-4)	0	0
2	2	3,6155(-3)	3,620(-3)	0	0
2	3	1,6801(-2)	1,680(-2)	0	0
2	4	1,6653(-2)	1,666(-2)	8,9821(-3)	9,9427(-3)
2	5	1,5068(-2)	1,507(-2)	7,8327(-2)	7,7366(-2)
2	6	1,3635(-2)	1,364(-2)	0	0
2	7	1,2337(-2)	1,234(-2)	0	0
2	8	8,6151(-3)	8,615(-3)	0	0
2	9	5,8402(-4)	5,839(-4)	0	0

Table 4. The linearly anisotropic component $\sigma_x(g' \to g, 1)$ of the inelastic transfer matrix for the 0.478 MeV level of ^7Li.

g'	g	TRAMA	NJOY
1	1	3,5646(-3)	3,562(-3)
1	2	1,2017(-2)	1,202(-2)
1	3	6,7865(-3)	6,785(-3)
1	4	1,4714(-3)	1,472(-3)
1	5	-2,8901(-3)	-2,891(-3)
1	6	-6,4420(-3)	-6,443(-3)
1	7	-6,2977(-3)	-6,298(-3)
1	8	-3,5407(-4)	-3,535(-4)
2	2	3,3575(-3)	3,361(-3)
2	3	1,3038(-2)	1,304(-2)
2	4	7,6829(-3)	7,687(-3)
2	5	1,8735(-3)	1,873(-3)
2	6	-2,8958(-3)	-2,897(-3)
2	7	-6,7804(-3)	-6,783(-3)
2	8	-7,1609(-3)	-7,161(-3)
2	9	-5,6225(-4)	-5,621(-4)

Table 5. Group structure used in the calculation of elastic scattering of ^{239}Pu.

Group	Lower energy (MeV)	Higher energy (MeV)
1	6,1160620	6,1672421
2	6,0653066	6,1160620
3	6,0149724	6,0653066
4	5,9650559	6,0149724

Table 6. The isotropic component $\sigma_x(g' \to g,\ 0)$ of the elastic transfer matrix of ^{239}Pu.

g'	g	TRAMA	NJOY	XLACS	MC^2
1	1	3,3656	3,366	3,3686	1,880
1	2	5,2051(-1)	5,203(-1)	5,2260(-1)	1,993
1	3	9,5879(-2)	9,585(-2)	9,0836(-2)	1,081(-1)
1	4	2,7928(-5)	2,785(-5)	0	1,256(-3)
2	2	3,3765	3,377	3,3795	1,886
2	3	5,2300(-1)	5,228(-1)	5,2509(-1)	2,000
2	4	9,5864(-2)	9,587(-2)	9,0814(-2)	1,083(-1)
3	3	3,3877	3,388	3,3907	1,893
3	4	5,2554(-1)	5,255(-1)	5,2761(-1)	2,007
4	4	3,3987	3,399	3,3971	1,900

Table 7. The linearly anisotropic component $\sigma_x(g' \to g,\ 1)$ of the elastic transfer matrix of ^{239}Pu.

g'	g	TRAMA	NJOY	XLACS	MC^2
1	1	3,1424	3,143	3,1454.	1,880
1	2	1,9883(-1)	1,986(-1)	2,0058(-1)	7,479(-2)
1	3	-6,2996(-2)	-6,299(-2)	-6,0840(-2)	-3,162(-1)
1	4	-2,7665(-5)	-2,759(-5)	0	-1,256(-3)
2	2	3,1522	3,152	3,1552	1,886
2	3	1,9968(-1)	1,995(-1)	2,0142(-1)	7,505(-2)
2	4	-6,2636(-2)	-6,264(-2)	-6,0483(-2)	-3,167(-1)
3	3	3,1623	3,162	3,1653	1,893
3	4	2,0053(-1)	2,005(-1)	2,0226(-1)	7,531(-2)
4	4	3,1720	3,172	3,1708	1,900

Table 8. The isotropic component $\sigma_x(g' \rightarrow g, 0)$ of the elastic transfer matrix of ^{27}Al.

g'	g	TRAMA	NJOY	XLACS
1	1	4,7788(-1)	4,779(-1)	4,7773(-1)
1	2	-2,0063(-2)	-2,007(-2)	-1,9117(-2)
2	2	6,2454(-1)	6,246(-1)	6,2413(-1)
2	3	-3,0460(-2)	-3,047(-2)	-2,7929(-2)
3	3	8,0954(-1)	8,096(-1)	8,0797(-1)
3	4	4,0843(-3)	4,083(-3)	5,4647(-3)
4	4	1,0634	1,063	1,0617
4	5	-3,1636(-2)	-3,164(-2)	-3,0285(-2)
5	5	3,3898(-1)	3,389(-1)	3,3813(-1)
5	6	-2,3081(-2)	-2,308(-2)	-2,3051(-2)
6	6	1,0026(-1)	1,003(-1)	9,9983(-2)
6	7	-1,3617(-2)	-1,362(-2)	-1,3600(-2)
7	7	5,1928(-2)	5,193(-2)	5,3383(-2)
7	8	-1,4343(-2)	-1,434(-2)	-1,5907(-2)
8	8	4,7044(-2)	4,704(-2)	4,7023(-2)
8	9	-1,3468(-2)	-1,347(-2)	-1,3470(-2)
9	9	4,4128(-2)	4,413(-2)	4,4080(-2)
9	10	-1,0550(-2)	-1,055(-2)	-1,0543(-2)
10	10	4,3949(-2)	4,395(-2)	4,3857(-2)
10	11	-1,0372(-2)	-1,037(-2)	-1,0334(-2)
11	11	4,3575(-2)	4,358(-2)	4,3577(-2)

Table 9. The linearly anisotropic component $\sigma_x(g' \rightarrow g,\ 1)$ of the elastic transfer matrix of ^{27}Al.

g'	g	TRAMA	NJOY	XLACS
1	1	6,3721(-1)	6,373(-1)	6,3476(-1)
1	2	1,2429(-1)	1,243(-1)	1,2676(-1)
2	2	8,5505(-1)	8,551(-1)	8,4984(-1)
2	3	2,2224(-1)	2,222(-1)	2,2743(-1)
3	3	1,3205	1,321	1,3157
3	4	1,8801(-1)	1,880(-1)	1,9287(-1)
4	4	3,0851	3,085	3,0843
4	5	1,3893(-1)	1,389(-1)	1,3983(-1)
5	5	5,0225	5,022	5,0224
5	6	6,3153(-2)	6,314(-2)	6,3213(-2)
6	6	3,4335	3,434	3,4334
6	7	4,2925(-2)	4,293(-2)	4,3264(-2)
7	7	1,4630	1,463	1,4579
7	8	4,5057(-2)	4,506(-2)	5,0115(-2)
8	8	1,3050	1,305	1,3049
8	9	4,2191(-2)	4,219(-2)	4,2294(-2)
9	9	1,3143	1,314	1,3143
9	10	3,2979(-2)	3,298(-2)	3,3015(-2)
10	10	1,3148	1,315	1,3149
10	11	3,2456(-2)	3,246(-2)	3,2402(-2)
11	11	1,3161	1,316	1,3159